JACS
JOURNAL OF THE AMERICAN CHEMICAL SOCIETY
Article
pubs.acs.org/JACS

Highly Luminescent InP/GaP/ZnS Nanocrystals and Their Application to White Light-Emitting Diodes

Sungwoo Kim,[†] Taehoon Kim,[†] Meejae Kang,[†] Seong Kwon Kwak,[‡] Tae Wook Yoo,[‡] Lee Soon Park,[§] Ilseung Yang,[∥] Sunjin Hwang,[∥] Jung Eun Lee,[∥] Seong Keun Kim,[∥] and Sang-Wook Kim*[,†]

[†]Department of Molecular Science and Technology, Ajou University, Suwon 443-749, Korea
[‡]Department of Sensor and Display, and [§]Department of Polymer Science, Kyungpook National University, Daegu 702-701, Korea
[∥]Department of Chemisty and WCU Department of Biophysics and Chemical Biology, Seoul National University, Seoul 151-747, Korea

Supporting Information

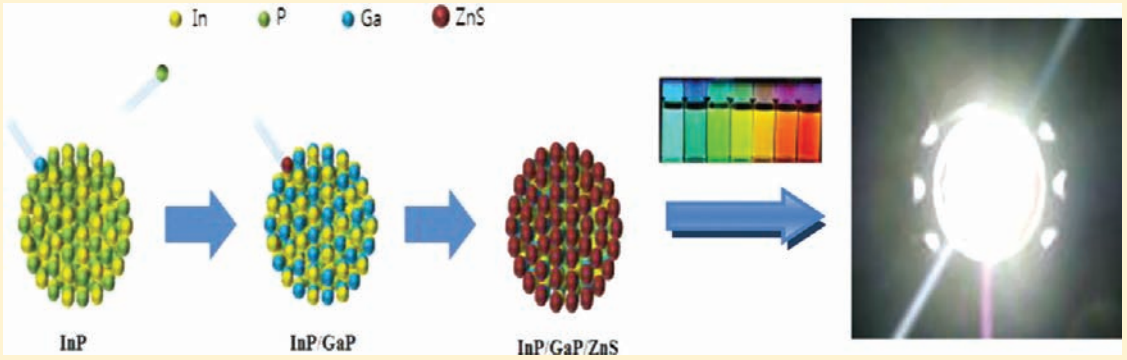

ABSTRACT: Highly stable and luminescent InP/GaP/ZnS QDs with a maximum quantum yield of 85% were synthesized by in situ method. The GaP shell rendered passivation of the surface and removed the traps. TCSPC data showed an evidence for the GaP shell. InP/GaP/ZnS QDs show better stability than InP/ZnS. We studied the optical properties of white QD-LEDs corresponding to various QD concentrations. Among various concentrations, the white QD-LEDs with 0.5 mL of QDs exhibited a luminous efficiency of 54.71 lm/W, *Ra* of 80.56, and CCT of 7864 K.

INTRODUCTION

The most interesting aspect of quantum dots (QDs) is the fact that they are bandgap-tunable materials by the size,[1] and, as a result, their fluorescence characteristics can also be varied. When compared to organic dyes, QDs have several optical merits, such as a narrow, tunable, and symmetric emission spectrum and outstanding photochemical stability. For this reason, QDs have found many applications in, for instance, light-emitting diodes (LEDs),[2] photovoltaic devices,[3] and biolabeling.[4] Extensive adoption of QDs by industry has been severely hindered, however, because they are highly toxic and thus pose a potential threat to the environment.[5] As an alternative to the most common CdSe QD, InP QD has been suggested as it shows a broadband emission spectrum comparable to that of CdSe, yet is much more environmentally compatible. Despite these advantages, InP QDs have not been put to practical use because they are prepared with more difficulty than CdSe, demonstrate poor quantum yields (QYs) below 1%, and exhibit weak photo- and chemical stability due to facile oxidation. To overcome these problems, it is important to control their surface properties, including defects.

It is well-known that the use of type-I core−shell structured QDs[6] containing a shell with a wider bandgap than that of their core results in improved QY by the surface passivation of the core by the shell. Many type-I core−shell QDs containing the InP core have recently been examined, including InP/ZnS,[7] InP/ZnSe,[8] and InP/ZnSSe.[9] However, because of the thin shell thickness, no satisfactory solution has been obtained that can guarantee a high QY and photochemical stability.

In this Article, we suggest a type-I structured InP/GaP/ZnS core/shell/shell QD. With the band offsets of bulk GaP located between InP and ZnS, our QD forms a type-I structure (Figure 1). The inner shell of GaP mitigates the effect of lattice mismatch between the InP core and the ZnS outer shell. These QDs show good photostability, aqueous dispersity, narrow emission band, and high QY, which would enable their application to white light-emitting diodes (WLEDs).

EXPERIMENTAL SECTION

Materials. These include indium(III) acetate (Aldrich, 99.99% metal basis), 1-dodecanethiol (Aldrich, 98+%), palmitic acid (TCI, 95%), zinc(II) acetate (Aldrich, 99.99% metal basis), oleic acid (TCI, 99%), 1-octadecene (Sigma Aldrich, 90%), tris(trimethylsilyl)-

Received: October 31, 2011
Published: February 3, 2012

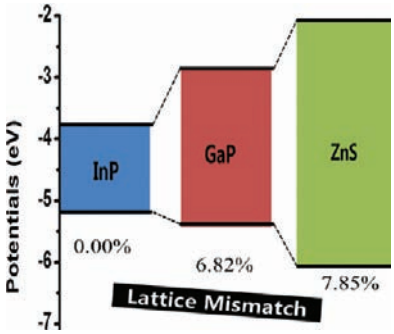

Figure 1. Band offsets and lattice mismatch of InP, GaP, and ZnS core/shell/shell materials.

phosphine 10 wt % hexane solution (Strem, 98%), gallium(III) chloride (Aldrich, ≥99.999% trace metals basis), and phosphatidylethanolamine (DSPE, Avanti).

Preparation of ZnInP Quantum Dot Core (All Reactions Are Under Inert Atmosphere). For the 530 nm Emitted Core. $In(OAc)_3$ (0.12 mmol, 35 mg), $Zn(OAc)_2$ (0.06 mmol, 12 mg), PA (0.36 mmol, 91 mg), and ODE (8 mL) were mixed in a 25 mL flask. The solution was heated to 110 °C and kept under a vacuum for 2 h. After degassing, $(TMS)_3P$ (0.06 mmol, 15 mg) in ODE (1 mL) was loaded into a syringe in a glovebox. The syringe contents were rapidly added to the flask at 300 °C and held at 230 °C for 2 h.

In Situ GaP/ZnS Multishell Formation. For the GaP shell coating, a precursor solution for GaP was prepared by mixing $GaCl_3$ (0.03 mmol, 5 mg) and oleic acid (0.1 mmol, 28 mg) in ODE (2 mL). This solution was added slowly to the ZnInP core solution at 200 °C. For the ZnS shell formation, $Zn(OAc)_2$ (0.3 mmol, 55 mg) was added to the reaction flask at room temperature and heated to 230 °C for 4 h. Finally, 1-dodecanethiol (0.5 mmol, 100 mg) was slowly injected into the flask and held for 2 h.

Process for White LED Fabricated with InP/GaP/ZnS Quantum Dots. LED chip bonding was implemented with a die bonder (West·Bond, Inc., CA) and a wire bonder (Kulicke and Soffa). The dual-component thermally curable silicone resin (OE-6630 A and B) was purchased from Dow Corning. The silicone-based encapsulants were made by mixing silicone resin parts A and B in a 1:4 weight ratio in mixing/degassing equipment made by the Thinky Co., Japan. The amount of YAG phosphor was kept constant at 6 wt % based on silicone resin, and InP/GaP/ZnS QDs were added in amounts from 4.0 to 7.0 g as toluene solutions. The phosphor-containing silicone encapsulant was injected in the LED lead frame by a dispenser and then thermally cured in a convection oven for 4 h according to the curing profile. Optical characteristics such as electroluminescence (EL), luminous efficiency, color temperature, CIE color coordinates, and color-rendering index (CRI) values of the WLEDs were evaluated using an integrating sphere with the Leos program.

Preparation of Phase Transfer Ligand. InP/GaP/ZnS QDs (8 mg) and phosphatidylethanolamine (40 mg, 5 equiv) were mixed in methylene chloride (2 mL) by bath sonication for 30 min. The mixed solution was evaporated by vacuum for 1 h at 50 °C. After methylene chloride was removed, 2−3 mL of water was added to yield a transparent solution.

Characterizations. Absorption spectra were measured by a Scinco PDA S-3100 UV/vis spectrophotometer. Emission spectra were obtained using a Jasco FP-6500 fluorescence spectrometer. Transmission electron microscopy (TEM) images and STEM-EDX were taken on a FEI Tecnai G2 F30 Super-Twin transmission electron microscope operating at 300 kV. X-ray diffraction (XRD) patterns were obtained using a Rigaku Ultima III diffractometer equipped with a rotating anode and a Cu Kα radiation source (λ = 0.15418 nm). Inductively coupled plasma-optical emission spectrometry (ICP-OES) was measured using the OPTIMA 5300DV, PerkinElmer (U.S.). Time-correlated single photon counting (TCSPC) was measured using the Nanofinder (λ = 405 nm). Zeta potentials were obtained using Otsuka Electronics ELS Z2.

RESULTS AND DISCUSSION

InP QDs were synthesized using zinc acetate ($Zn(OAc)_2$), indium acetate ($In(OAc)_3$), tris(trimethylsilyl)phosphine

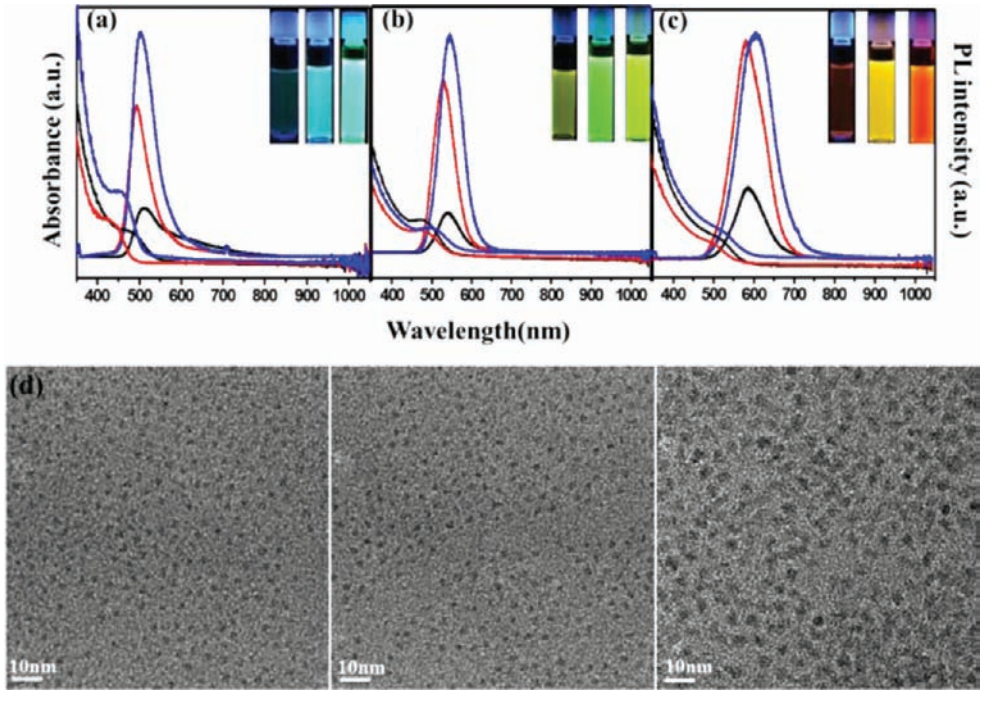

Figure 2. Absorption and photoluminescence spectra of InP (black) cores, InP/GaP (red) core−shells, and InP/GaP/ZnS (blue) core−shell−shell at each wavelength. Insets: Photograph of InP (left), InP/GaP (middle), and InP/GaP/ZnS (right) (a−c). (d) TEM image of InP (left), InP/GaP (middle), and InP/GaP/ZnS (right).

dx.doi.org/10.1021/ja210211z | J. Am. Chem. Soc. 2012, 134, 3804−3809

($(TMS)_3P$), and palmitic acid (PA) as precursors and stabilizer, which is similar to the methodology reported by Nann et al.[7f] A conventionally synthesized InP core exhibits weak photoluminescence due to surface traps. As a solution to this problem, an octadecene (ODE) solution of $Zn(OAc)_2$, $In(OAc)_3$, and PA was prepared, and a $(TMS)_3P$–ODE stock solution was rapidly injected at 300 °C. As a result, the QY increased to 15% because the Zn^{2+} ions attached to the surface and partially removed the surface traps. Some reports[7f,i] suggested that zinc carboxylates without dodecanethiol resulted in the improvement of the optical properties by lattice doping and In(Zn)P alloy formation. The GaP shell was applied to the core by adding a gallium–oleate complex solution. For example, InP QDs with an emission peak at 510 nm were prepared using 0.04 mmol of $Zn(OAc)_2$, 0.04 mmol of $In(OAc)_3$, and 0.02 mmol of $(TMS)_3P$ in 3 mL of ODE. To prepare the GaP shell, a Ga–oleate complex (0.02 mmol) solution was added dropwise to the InP core solution at 210 °C without adding more phosphine precursor. The detailed procedures are described in the Experimental Section. Three InP cores with emission peaks at 515, 540, and 590 nm were chosen for the synthesis of the InP/GaP core/shell structures. By adding a Ga–oleate solution, we observed a blue shift of 5–15 nm in emission so that the peaks shifted to 490, 530, and 585 nm, respectively (Figure 2a–c). Moreover, the QY increased further to 15–35%. Similarly, the absorption peaks were also blue-shifted. Two hypotheses can be proposed to explain these experimental results. The first is surface adsorption of the Ga^{3+} ion on the InP cores; however, the residual Ga content in this case should be very small and irregular after a workup process. Our experiments showed reproducible Ga to In ratios of 10–15%. As an alternative, a cation exchange[10] reaction between In^{3+} and Ga^{3+} can be considered, and we note that similar phenomena have been reported previously,[10e] although the cations were different. An exchange reaction between In^{3+} and Ga^{3+} is highly likely, considering their common zinc-blende structures of similar lattice parameters (InP, 5.86 Å; GaP, 5.45 Å), and the similar ionic radii of Ga^{3+} (0.75 Å) and In^{3+} (0.81 Å). If Ga^{3+} ions effectively replace In^{3+} ions near the surface, a structurally congruent InP/GaP core/shell structure could be formed (Scheme 1). The reduction in size of the InP core after coating

Scheme 1. Cation Exchange by Ga^{3+} on InP Core Surface

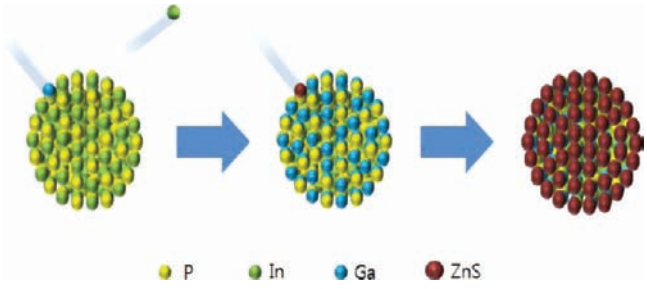

with a GaP shell due to cation exchange can explain the blue shifts in emission and absorption. The same blue shift was observed when the Ga precursors were added to the InP solution after a workup process. This fact means that the reaction between Ga and the unreacted phosphine precursor was negligible. The optimized amount of Ga precursors was a quarter of the amount of In, which resulted in the most highly improved optical properties. Excessive use of Ga precursors exhibited translucent scattering of the solution and reduced the quantum efficiency.

Finally, we coated an additional shell of ZnS to obtain more stable QDs, by using $Zn(OAc)_2$ and 1-dodecanethiol (DDT) as the precursors, which were added to an InP/GaP core/shell solution and maintained at 230 °C. The detailed formation step of the ZnS shell can be found in Supporting Information S6. As a result, an improved QY and consistent red shifts in emission were observed (from 490 to 505 nm, 530 to 555 nm, and 590 to 615 nm). The multishell structure led to improved QY of 24% (Figure 1a), 85% (Figure 1b), and 58% (Figure 1c), which were obtained by comparison with Coumarin 153 (53% in ethanol), Coumarin 110 (91% in ethanol), and Rhodamin 6G (95% in ethanol). Figure 2 shows the photoluminescence spectrum, absorption spectrum, and actual photographs of the InP core, InP/GaP core/shell, and InP/GaP/ZnS core/shell/shell at each wavelength, respectively. Figure 2d–f shows the transmission electron microscopy (TEM) images of the InP core, InP/GaP core/shell, and InP/GaP/ZnS core/shell/shell structures, respectively. The InP core has a mean diameter of 3.1 nm (Figure 1e) and an emission peak in the range of 515–595 nm. The tuning of the emission wavelength was enabled by controlling the precursor concentration. The diameters of the InP/GaP core/shell and InP/GaP/ZnS core/shell/shell were 3.3 and 5.0 nm, respectively (Figure 1e and f). High-resolution TEM (HR-TEM) images showed that the core/shell/shell QDs have a single-crystalline structure, which indicates epitaxial growth of shell components due to the common zinc-blende structure and similar lattice parameters between InP (5.86 Å), GaP (5.45 Å), and ZnS (5.40 Å) (Supporting Information S1). Scanning transmission electron microscopy-electron dispersive X-ray spectroscopy (STEM-EDX) data showed particles with atomic identity of InP/GaP/ZnS (Supporting Information S2). Figure 3a shows the powder X-ray diffraction (XRD) patterns that are indexed to the (111), (220), and (311) planes of the zinc-blende structure of the InP core, InP/GaP core/shell, and InP/GaP/ZnS core/shell/shell, respectively. The slight peak shifts between InP and InP/GaP and the larger peak shift between InP/GaP and InP/GaP/ZnS indicate the existence of GaP and ZnS shell structures. Figure 3b shows the high-resolution X-ray photoelectron spectroscopy (XPS) spectrum of InP/GaP. Ga_{2P3} peaks were observed at about 1180.60 eV, which represents the binding of Ga in the GaP shell. The presence of Ga was confirmed by inductively coupled plasma atomic emission spectroscopy (ICP-AES). The two InP/GaP samples that showed emissions at 530 and 590 nm had similar In/Ga molar ratios of 6.2/1. Meanwhile, InP/GaP/ZnS samples had an increased In/Ga molar ratio of 7.5/1, which indicates a decreased Ga content. The reason may be related to the etching effect of Zn^{2+} during the ZnS shell coating, which was previously reported for InP/ZnS.[7h]

To investigate the dynamical features of our QDs, we probed the temporal decay of the photoexcited state by time-correlated single photon counting (TCSPC). Figure 3b shows that the temporal decay of all samples is biexponential in nature. The decay curves were fitted accordingly with the following function, and the fitting parameters are given in Figure 3b:

$$f(t) = a_1\exp(-t/t_1) + a_2\exp(-t/t_2), \text{ where} a_1 + a_2 = 1$$

We note that the amplitude for the slow decay component (a_2) is lowest for the InP core (0.30), but increases drastically for the InP/GaP core/shell (0.68), and even further for the InP/GaP/ZnS core/shell/shell structure (0.88), which is

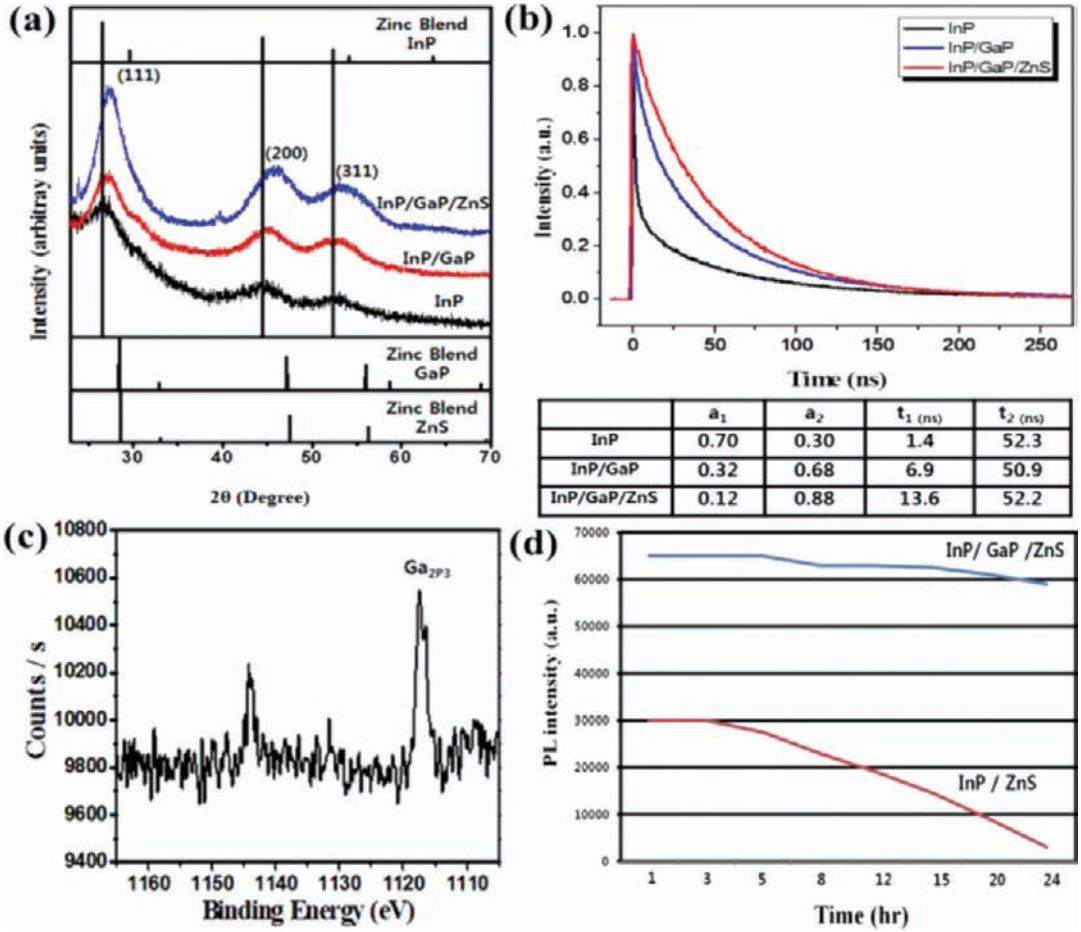

	a_1	a_2	$t_{1\ (ns)}$	$t_{2\ (ns)}$
InP	0.70	0.30	1.4	52.3
InP/GaP	0.32	0.68	6.9	50.9
InP/GaP/ZnS	0.12	0.88	13.6	52.2

Figure 3. (a) XRD patterns of InP, InP/GaP, and InP/GaP/ZnS and reflections of zinc blende bulk InP, GaP, and ZnS. (b) TCSPC data of InP, InP/GaP, and InP/GaP/ZnS. (c) High-resolution XPS spectra of InP/GaP from Ga_{2P3}. (d) Thermal stability of the InP/ZnS and InP/GaP/ZnS, which were tested at 150 °C.

readily explained by increase in PL by shell passivation. It is widely known that the surfaces of colloidal QDs play important roles in carrier relaxation and recombination processes.[13] Shell passivation efficiently removes the carrier quenching defects on the surface, thereby increasing the rate of radiative recombination. For quantum dots with core/shell structures, the atoms of the core and the shell epitaxially bond together with minimal defects.[14d] The individual LUMO of core and shell will have strong interactions, in which the core/shell LUMO will be largely delocalized throughout the reconstructed structure.[14d] The fast decay component is associated with the facile decay of carrier population due to internal core state recombination.[13a,14] It was proposed that the hole could be excited to surface localized states at the same energy as that of the internal core states because of their strong mixing.[14a,15] As the passivation of InP increases, the lifetime of the fast component gradually increases due to strong mixing.

Supporting Information S3 reports another comparative study, in which InP, InP/Zn^{2+}, and InP/ZnS QDs, which are intermediates for InP/ZnS core/shell QDs, were measured. Interestingly, InP/Zn^{2+} has a high contribution of the fast component, while InP/GaP shows a high contribution of the slow component, indicating that they are different structures: one results from cation passivating, and the other results from shell passivating. This is also strong evidence for the InP/GaP core/shell structure.

The heat stabilities of the InP/ZnS and InP/GaP/ZnS QDs were also examined by watching the change in photoluminescence (PL) intensity over time upon thermal aging at 150 °C. Figure 3d shows that the PL intensity of the freshly prepared InP/GaP/ZnS QDs decreased only slightly (by ~10% in 24 h), while that of the InP/ZnS QDs showed a sharp decline after 3 h and ultimately by more than 90% in 24 h. This demonstrates that the current multishell QDs of InP/GaP/ZnS have a much superior thermal stability over InP/ZnS QDs that were synthesized by our previously reported method.[7h] We were also able to transfer the QDs from an organic to an aqueous phase by ligand exchange, which produced highly luminescent and water-dispersible QDs (Supporting Information S4). The fluorescent QY after phase transfer decreased from 80% to 70%. In an additional stability test, we examined the PL intensity change of the InP/GaP/ZnS QDs under irradiation with a 254 nm UV lamp at a small distance of 10 cm for 100 h. No significant changes were detected in the PL intensity during this aging time (Supporting Information S5), which again confirms that our multishell structure is highly stable. It is likely that multiple shells effectively reduce the surface-dangling bonds that act as trap sites for charge carriers and reduce fluorescence.[12]

Recently, LEDs as solid-state light devices have attracted considerable interest because of their environmentally friendly properties, long lifetimes, low power consumption, high efficiency, and fast response times. Generally, there have been

dx.doi.org/10.1021/ja210211z | J. Am. Chem. Soc. 2012, 134, 3804−3809

WLEDs using InGaN blue chips with yellow-emitting Ce^{3+}-doped $Y_3Al_5O_{12}$ (YAG:Ce) phosphors.[2p] Although this WLED system having high luminous efficacy and good stability has been commercialized, it is difficult to obtain a high color-rendering index (*Ra*) due to deficiencies in the green and red ranges. To solve these problems, Wu et al. attempted to use green/red phosphors to enhance the luminous efficacy to 15 lm/W and the *Ra* index to 92.2 at 5937 K.[2j] It was reported that Cd-based QDs of core, core/shell, and core/shell/shell could be applied to WLEDs. Jang et al. developed a high efficiency WLED with a high *Ra* of 90.1 at 8864 K using green- and yellow-emitting $Sr_3SiO_5:Ce^{3+}/Li^+$ and CdSe QDs.[2m] Lim et al. reported a WLED using CdSe/CdS/ZnS QDs without a phosphor source.[2o] In addition, Jang et al. reported a WLED for backlight units using CdSe/ZnS/CdSZnS green QDs and CdSe/CdS/ZnS/CdSZnS red QDs color converters based on blue LEDs.[2e] Ziegler et al. reported a blue LED using silica-coated InP/ZnS QDs with a $Sr_{0.94}Al_2O_4:Eu_{0.06}$ green phosphor and YAG:Ce yellow phosphor, which showed a luminous efficacy of 15 lm/W and an *Ra* index of 86 at 3900 K.[2h]

We applied red-emitting InP/GaP/ZnS QDs, which were mixed with a YAG:Ce phosphor, to a WLED. To make a WLED module with high color-rendering properties, InP/GaP/ZnS QDs and YAG:Ce phosphors were mixed with silicon resins in a toluene solvent. After removing the solvent, the YAG−QD silicon mixture was dropped on InGaN blue LED chips and cured at 150 °C for 4 h. The detailed procedure for preparing the QD-LED is described in the Experimental Section. Figure 4b shows a schematic illustration of a YAG phosphor-QD-based WLED.

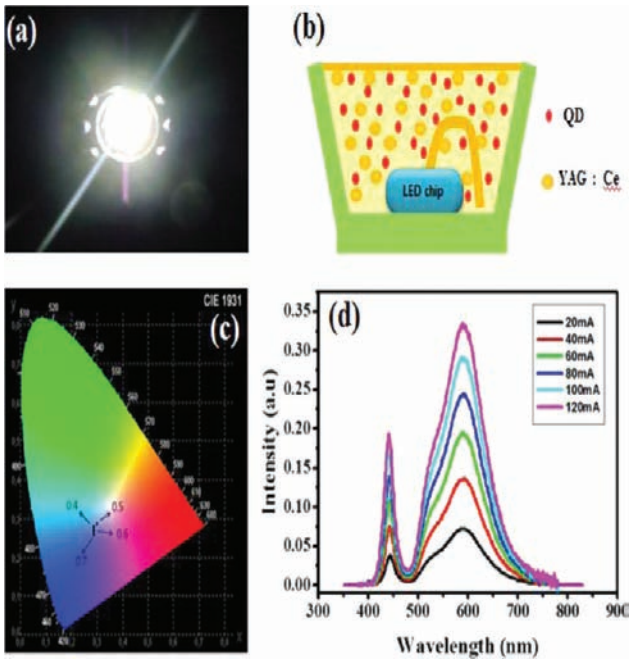

Figure 4. (a) Photograph of white LED using InP/GaP/ZnS QDs. (b) Schematic illustration of a YAG phosphor-QDs based WLED. (c) CIE diagram of the corresponding QD concentration. (d) Emission spectra of a WLED prototype at currents from 20 to 120 mA.

Figure 4c shows the Commission Internationale de l'Eclairage (CIE) chromaticity color coordinates that were (0.2938, 0.27058), (0.3034, 0.2881), (0.2933, 0.2676), and (0.2915, 0.2611), corresponding to the QD amounts of 0.4, 0.5, 0.6, and 0.7 mL, respectively. Moreover, a color temperature (CCT) was exhibited at 9503, 7864, 9860, and 10598 K. As the QD amount increased to 0.5 mL, the color of the emitting light shifted from yellow to near-white of a suitable WLED, and the CCT moved to warm white due to an increased red color region. However, at amounts of more than 0.5 mL of QDs, the CIE color coordinates (*x*,*y*) decreased and the CCT moved to the cool white region. At a working current of 120 mA, the luminous efficacies were 58.47, 54.71, 51.66, and 47.21 lm/W, corresponding to the QD amounts of 0.4, 0.5, 0.6, and 0.7 mL, respectively. As the QD amounts increased, the luminous efficacy showed a reduced tendency due to diminution of the luminous flux by light loss. The *Ra* index improved from 79.72 to 80.56 (Supporting Information S7). Figure 4a shows a photograph of a WLED using 0.5 mL of QDs. Figure 4d shows the emission spectra of InP/GaP/ZnS QDs with a YAG-based WLED when operated from 20 to 120 mA bias currents. There are three emission peaks at 455, 535, and 615 nm. The PL of InP/GaP/ZnS shows an orange emission at 595 nm. On the other hand, the emission by the WLED was observed at 610 nm. The difference was a result of the agglomeration of InP/GaP/ZnS QDs in the silicon resin, and the effect of the changed surface and surrounding medium, which affected the excitonic binding energy of the QDs to some extent.[11]

CONCLUSION

Highly stable and luminescent Cd-free InP/GaP/ZnS QDs with a maximum quantum yield of 85% were synthesized by the in situ method. The GaP shell rendered passivation of the surface and removed the traps. TEM images showed a size change, the powder XRD (PXRD) pattern revealed a peak shift, and the TCSPC component showed an evidence for the GaP shell. Because of the GaP shell, we assume that InP/GaP/ZnS QDs possess better stability than InP/ZnS. We studied the optical properties of white QD-LEDs corresponding to various QD concentrations. Among various concentrations, the white QD-LEDs with 0.5 mL exhibited a luminous efficiency of 54.71 lm/W, *Ra* of 80.56, and CCT of 7864 K at the color coordinate (0.3034, 0.2881). These would possibly be suitable for white illumination source applications.

ASSOCIATED CONTENT

Supporting Information

Detailed experimental procedure, the HR-TEM image and STEM-EDX of InP/GaP/ZnS QDs, and TCSPC data of InP/ZnS core/shells QDs. Absorption and emission spectra during ZnS shell formation. Surface and thermal stability data and white LED data of InP/GaP/ZnS NCs. Zeta Potential data of InP/Zn^{2+}, InP/GaP, and elemental composition and standard deviation according to the EDX data of the different sized InP/GaP/ZnS. This material is available free of charge via the Internet at http://pubs.acs.org.

AUTHOR INFORMATION

Corresponding Author

swkim@ajou.ac.kr

Notes

The authors declare no competing financial interest.

ACKNOWLEDGMENTS

This work was supported by the National Research Foundation of Korea (NRF) grant no. 2009-0067322, the Global Frontier

R&D Program for Multiscale Energy System, the Priority Research Centers Program (2009-0093826), and the Industrial Core Technology Development Program funded by the Ministry of Knowledge Economy (no. 10035274), Republic of Korea.

REFERENCES

(1) (a) Murray, C. B.; Norris, D. J.; Bawendi, M. G. *J. Am. Chem. Soc.* **1993**, *115*, 8706−8715. (b) Bawendi, M. G.; Steigerwald, M. L.; Brus, L. E. *Annu. Rev. Phys. Chem.* **1990**, *41*, 477−496. (c) Alivisatos, A. P. *J. Phys. Chem.* **1996**, *100*, 13226−13239.

(2) (a) Hu, J.; Li, L.; Yang, W.; Manna, L.; Wang, L.; Alivisatos, A. P. *Science* **2001**, *292*, 2060−2063. (b) Li, Y.; Rizzo, A.; Cingolani, R.; Gigli, G. *Adv. Mater.* **2006**, *18*, 2545−2548. (c) Anikeeva, P. O.; Halpert, J. E.; Bawendi, M. G. *Nano Lett.* **2007**, *7*, 2196−2200. (d) Lee, J.; Sundar, V. C.; Heine, J. R.; Bawendi, M. G.; Jensen, K. F. *Adv. Mater.* **2000**, *12*, 1102−1105. (e) Jang, E.; Jun, S.; Jang, H.; Lim, J.; Kim, B.; Kim, Y. *Adv. Mater.* **2010**, *22*, 3076−3080. (f) Chen, H. S.; Hsu, C. K.; Hong, H. Y. *IEEE Photonics Technol. Lett.* **2006**, *18*, 193−195. (g) Dai, Q.; Duty, C. E.; Hu, M. Z. *Small* **2010**, *6*, 1577−1588. (h) Ziegler, J.; Xu, S.; Kucur, E.; Meister, F.; Batentschuk, M.; Gindele, F.; Nann, T. *Adv. Mater.* **2008**, *20*, 4068−4073. (i) Woo, J. Y.; Kim, K. N.; Jeong, S.; Han, C.-S. *Nanotechnology* **2010**, *21*, 495704. (j) Wu, H.; Zhang, X.; Guo, C.; Xu, J.; Wu, M.; Su, Q. *IEEE Photonics Technol. Lett.* **2005**, *17*, 1160−1162. (k) Ali, M.; Chattopadhyay, S.; Nag, A.; Kumar, A.; Sapra, S.; Chakraborty, S.; Sarma, D. D. *Nanotechnology* **2007**, *18*, 075401:1−4. (l) Nizamoglu, S.; Ozel, T.; Sari, E.; Demir, H. V. *Nanotechnology* **2007**, *18*, 065709. (m) Jang, H. S.; Yang, H.; Kim, S. W.; Han, J. Y.; Lee, S. G.; Jeon, D. Y. *Adv. Mater.* **2008**, *20*, 2696−2702. (n) Kwon, B. H.; Jang, H. S.; Yoo, H. S.; Kim, S. W.; Kang, D. S.; Maeng, S.; Jang, D. S.; Kim, H.; Jeon, D. Y. *J. Mater. Chem.* **2011**, *21*, 12812−12818. (o) Lim, J.; Jun, S.; Jang, E.; Bail, H.; Kim, H.; Cho, J. *Adv. Mater.* **2007**, *19*, 1927−1932. (p) Nakamura, S.; Fasol, G. *The Blue Laser Diode: GaN Based Light Emitters and Laser*; Springer: Berlin, 1996; pp 216−221.

(3) (a) Steinhagen, C.; Panthani, M. G.; Akhavan, V.; Goodfellow, B.; Koo, B.; Kogel, B. A. *J. Am. Chem. Soc.* **2009**, *131*, 12554−12555. (b) Beecher, P.; Quinn, A. J.; Shevchenko, E. V.; Weller, H.; Redmond, G. *Nano Lett.* **2004**, *4*, 1289−1293. (c) Ma, W.; Luther, J. M.; Zheng, H.; Wu, Y.; Alivisatos, A. P. *Nano Lett.* **2009**, *9*, 1699−1703. (d) Zhao, N.; Osedach, T. P.; Chang, L. Y.; Geyer, S. M.; Wanger, D. D.; Binda, M. T.; Arango, A. C.; Bawendi, M. G.; Bulovic, V. *ACS Nano* **2010**, *4*, 3743−3752. (e) Li, L.; Coates, N.; Moses, D. *J. Am. Chem. Soc.* **2010**, *132*, 22−23. (f) Guo, Q.; Hillhouse, H. W.; Agrawal, R. *J. Am. Chem. Soc.* **2009**, *131*, 11672−11673. (g) Leschkies, K. S.; Beatty, T. J.; Kang, M. S.; Norris, D. J.; Aydil, E. S. *ACS Nano* **2009**, *3*, 3638−3648. (h) Shao, S.; Liu, F.; Xie, Z.; Wang, L. *J. Phys. Chem. C* **2010**, *114*, 9161−9166. (i) Im, S. H.; Lee, Y. H.; Seok, S. I.; Kim, S. W.; Kim, S.-W. *Langmuir* **2010**, *26*, 18576−18580.

(4) (a) Bruchez, M. Jr.; Moronne, M.; Gin, P.; Weiss, S.; Alivisatos, A. P. *Science* **1998**, *281*, 2013−2016. (b) Chan, W. C. W.; Nie, S. *Science* **1998**, *281*, 2016−2018. (c) Medintz, I. L.; Uyeda, H. T.; Goldman, E. R.; Mattoussi, H. *Nat. Mater.* **2005**, *4*, 435−436. (d) Yang, J.; Lee, C.-H.; Ko, H.-J.; Suh, J.-S.; Yoon, H.-G.; Lee, K.; Huh, Y.-M.; Haam, S. *Angew. Chem., Int. Ed.* **2007**, *46*, 8836−8839. (e) Kim, S.; Lim, Y. T.; Soltesz, E. G.; De Grand, A. M.; Lee, J.; Nakayama, A.; Parker, J. A.; Mihaljevic, T.; Laurence, R. G.; Dor, D. M.; Cohn, L. H.; Bawendi, M. G.; Frangioni, J. V. *Nat. Biotechnol.* **2004**, *22*, 93−97. (f) Allen, P. M.; Liu, W.; Chauhan, V. P.; Lee, J.; Ting, A. Y.; Fukumura, D.; Jain, R. K.; Bawendi, M. G. *J. Am. Chem. Soc.* **2010**, *132*, 470−471.

(5) (a) Hardman, R. *Environ. Health Perspect.* **2006**, *114*, 165−172. (b) Kirchner, C.; Liedl, T.; Kudera, S.; Pellegrino, T.; Javier, A. M.; Gaub, H. E.; Stolzle, S.; Fertig, N.; Parak, W. J. *Nano Lett.* **2005**, *5*, 331−338.

(6) Dabbousi, B. O.; Rodriguez-Viejo, J.; Mikulec, F. V.; Heine, J. R.; Mattoussi, H.; Ober, R.; Jensen, K. F.; Bawendi, M. G. *J. Phys. Chem. B* **1997**, *101*, 9463−9475.

(7) (a) Haubold, S.; Haase, M.; Kornowski, A.; Weller, H. *ChemPhysChem* **2001**, *5*, 331−334. (b) Peng, X.; Battaglia, D. *Nano Lett.* **2002**, *2*, 1027−1030. (c) Talapin, D. V.; Gaponik, N.; Borchert, H.; Rogach, A. L.; Haase, M.; Weller, H. *J. Phys. Chem. B* **2002**, *106*, 12659−12663. (d) Xu, S.; Kumar, S.; Nann, T. *J. Am. Chem. Soc.* **2006**, *128*, 1054−1055. (e) Xie, R.; Battaglia, D.; Peng, X. *J. Am. Chem. Soc.* **2007**, *129*, 15432−15433. (f) Xu, S.; Ziegler, J.; Nann, T. *J. Mater. Chem.* **2008**, *18*, 2653−2656. (g) Li, L.; Reiss, P. *J. Am. Chem. Soc.* **2008**, *130*, 11588−11589. (h) Ryu, E.; Kim, S.; Jang, E.; Jun, S.; Jang, H.; Kim, B.; Kim, S.-W. *Chem. Mater.* **2009**, *21*, 573−575. (i) Thuy, U. T. D.; Reiss, P.; Liem, N. Q. *Appl. Phys. Lett.* **2010**, *97*, 193104.

(8) Kim, M. R.; Chung, J. H.; Lee, M.; Lee, S.; Jang, D. J. *J. Colloid Interface Sci.* **2010**, *350*, 5−9.

(9) Lim, J.; Bae, W. K.; Lee, D.; Nam, M. K.; Jung, J.; Lee, C.; Char, K.; Lee, S. *Chem. Mater.* **2011**, *23*, 4459−4463.

(10) (a) Son, D. H.; Hughes, S. M.; Yin, Y.; Alivisatos, A. P. *Science* **2004**, *306*, 1009−1012. (b) Chan, E. M.; Marcu, M. A.; Fakra, S.; Naggar, M. E.; Mathies, R. A.; Alivisatos, A. P. *J. Phys. Chem. A* **2007**, *111*, 12210−12215. (c) Robinson, R. D.; Sadtler, B.; Demchenko, D. O.; Erdonmez, C. K.; Wang, L.; Alivisatos, A. P. *Science* **2007**, *317*, 355−358. (d) Wark, S. E.; Hsia, C.; Son, D. H. *J. Am. Chem. Soc.* **2008**, *130*, 9550−9555. (e) Park, J.; Kim, S.-W. *J. Mater. Chem.* **2011**, *21*, 3745−3750.

(11) Song, H.; Lee, S. *Nanotechnology* **2007**, *18*, 255202(1)−(4).

(12) Talapin, D. V.; Mekis, I.; Götzinger, S.; Kornowski, A.; Renson, O.; Weller, H. *J. Phys. Chem. B* **2004**, *108*, 18826−18831.

(13) (a) Klimov, V. I.; McBranch, D. W.; Leatherdale, C. A.; Bawendi, M. G. *Phys. Rev. B* **1999**, *60*, 13740−13749. (b) Wang, X. Y.; Qu, L. H.; Zhang, J. Y.; Peng, X.; Xiao, M. *Nano Lett.* **2003**, *3*, 1103−1106.

(14) (a) Bawendi, M. G.; Carroll, P. J.; Wilson, W. L.; Brus, L. E. *J. Chem. Phys.* **1992**, *96*, 946−954. (b) Zhang, J. Y.; Wang, X. Y.; Xiao, M. *Opt. Lett.* **2002**, *27*, 1253−1255. (c) Wang, X. Y.; Zhang, J. Y.; Nazzal, A.; Darragh, M.; Xiao, M. *Appl. Phys. Lett.* **2002**, *81*, 4829−4831. (d) Peng, X.; Schlam, M. C.; Kadavanich, A. V.; Alivisatos, A. P. *J. Am. Chem. Soc.* **1997**, *119*, 7019.

(15) Carstensen, H.; Claessen, R.; Manzke, R.; Skibowski, M. *Phys. Rev. B* **1990**, *41*, 9880−9885.